J. Fluid Mech. (1995), *vol.* 305, *pp.* 281–305

Compressible magnetoconvection in three dimensions: planforms and nonlinear behaviour

By P.C. MATTHEWS†, M.R.E. PROCTOR AND N.O. WEISS

Department of Applied Mathematics and Theoretical Physics,
University of Cambridge, Silver Street, Cambridge CB3 9EW, UK

(Received 11 October 1994 and in revised form 1 September 1995)

Convection in a compressible fluid with an imposed vertical magnetic field is studied numerically in a three-dimensional Cartesian geometry with periodic lateral boundary conditions. Attention is restricted to the mildly nonlinear regime, with parameters chosen first so that convection at onset is steady, and then so that it is oscillatory.

Steady convection occurs in the form of two-dimensional rolls when the magnetic field is weak. These rolls can become unstable to a mean horizontal shear flow, which in two dimensions leads to a pulsating wave in which the direction of the mean flow reverses. In three dimensions a new pattern is found in which the alignment of the rolls and the shear flow alternates.

If the magnetic field is sufficiently strong, squares or hexagons are stable at the onset of convection. Both the squares and the hexagons have an asymmetrical topology, with upflow in plumes and downflow in sheets. For the squares this involves a resonance between rolls aligned with the box and rolls aligned diagonally to the box. The preference for three-dimensional flow when the field is strong is a consequence of the compressibility of the layer – for Boussinesq magnetoconvection rolls are always preferred over squares at onset.

In the regime where convection is oscillatory, the preferred planform for moderate fields is found to be alternating rolls – standing waves in both horizontal directions which are out of phase. For stronger fields, both alternating rolls and two-dimensional travelling rolls are stable. As the amplitude of convection is increased, either by decreasing the magnetic field strength or by increasing the temperature contrast, the regular planform structure seen at onset is soon destroyed by secondary instabilities.

1. Introduction

The original motivation for studying the interaction between magnetic fields and convection came from astrophysics. Sunspots, and starspots, are dark because normal convection is impeded by a strong magnetic field. High-resolution observations, coupled with theoretical advances, are gradually leading to a clearer understanding of convective transport both in the dark umbra of a sunspot, where the magnetic field is essentially vertical, and in the filamentary penumbra, where the field is inclined (Thomas & Weiss 1992). Meanwhile, magnetoconvection has become an important topic in its own right, as a prototype of double-diffusive behaviour. The competition between a superadiabatic thermal stratification and the stabilizing effect

† Present address: Department of Theoretical Mechanics, University of Nottingham, University Park, Nottingham NG7 2RD, UK.

of the magnetic field gives rise to a rich variety of spatiotemporal behaviour. Since the Lorentz force is quadratic, magnetoconvection exhibits an even wider range of solutions than thermosolutal or binary convection, or convection in a rotating system. Slow magnetoacoustic oscillations can be thermally excited, yielding both travelling and standing waves, while shearing instabilities lead to travelling, modulated and pulsating waves (Weiss 1991; Proctor 1992; Matthews *et al.* 1993). It is fortunate that recent developments in nonlinear dynamics have made it possible for us to analyse the competition between different planforms and patterns of time-dependent motion.

Early investigations of magnetoconvection employed the Boussinesq approximation. Linear theory shows that behaviour depends critically on the ratio, ζ, of the magnetic to the thermal diffusivity: if $\zeta > 1$ convection appears as a direct instability (at a pitchfork bifurcation) giving rise to steady motion, but if $\zeta < 1$, as at the surface of the Sun, and the field is sufficiently strong then convection sets in as an oscillatory instability (at a Hopf bifurcation) leading to periodic solutions (Chandrasekhar 1961). In two dimensions, with mirror-symmetry imposed at the lateral boundaries, the oscillations take the form of standing waves; nonlinear interactions between standing waves and steady solutions have been thoroughly investigated, using a combination of analytical and numerical techniques (Proctor & Weiss 1982). Once the lateral boundary conditions are relaxed, both standing waves and travelling waves appear together at the oscillatory bifurcation and weakly nonlinear theory can be used to determine which solution is preferred (Matthews & Rucklidge 1993). Numerical experiments on two-dimensional compressible magnetoconvection have revealed a variety of steady and time-dependent patterns of behaviour (Hurlburt & Toomre 1988; Hurlburt *et al.* 1989; Weiss *et al.* 1990; Proctor *et al.* 1994; Brownjohn *et al.* 1995). Stable travelling waves can appear either at the initial bifurcation or in a secondary bifurcation, where the mirror-symmetry of steady rolls is broken. In the latter case, shearing instabilities may develop to yield a pulsating wave (Matthews *et al.* 1993).

It is not obvious which features – if any – of two-dimensional convection will survive once three-dimensional perturbations are admitted. Turbulent Rayleigh–Bénard convection in a three-dimensional compressible layer has already been simulated with considerable success (Stein & Nordlund 1989; Cattaneo *et al.* 1991) and the computational results bear a close resemblance to images of the solar granulation (Spruit, Nordlund & Title 1990). In this paper we embark on a systematic study of three-dimensional compressible magnetoconvection. Once again we follow the approach that has proved successful in two-dimensional investigations. Different patterns of nonlinear behaviour are isolated through numerical experiments in an idealized configuration with widely varying parameters. We begin near the initial bifurcation, where computations can be compared with linear and weakly nonlinear analytical results, and explore behaviour as the relevant instability parameter (the Rayleigh number) is progressively increased. This gradual but systematic approach differs from other, more ambitious simulations of turbulent magnetoconvection (e.g. Brandenburg *et al.* 1990; Nordlund & Stein 1990; Nordlund *et al.* 1992; Vainshtein *et al.* 1993; Nordlund, Galsgaard & Stein 1994).

We shall be concerned here only with mildly nonlinear behaviour in a shallow stratified layer. Our aim is to exhibit, classify and relate the different planforms that arise for steady and periodic magnetoconvection. We do find stable two-dimensional rolls – as steady solutions and travelling, modulated or pulsating waves – but there is also a new range of three-dimensional solutions. In addition, we study transitions between different spatiotemporal patterns in the nonlinear regime. These

transitions can only be described if computations are related to low-order model systems, comprising a limited number of coupled nonlinear ordinary differential equations. Such low-order models, whether normal form equations or more arbitrary evolution equations, can be solved precisely and then interpreted in terms of nonlinear dynamics. They are an essential tool in analysing the numerical results; without recent developments in bifurcation theory it would be impossible to make sense of the many solutions that are found.

In what follows we shall describe and illustrate the different planforms and types of time-dependent behaviour that appear as the relevant parameters are varied over a wide range. Computations will be carried out in domains which are either square or rectangular in the horizontal plane and have periodic boundary conditions. We shall also analyse transitions from one spatiotemporal pattern to another. Three-dimensional runs are much more difficult to analyse than two-dimensional results, which can be fully represented on a plane. Time-dependent solutions are best displayed as colour videos, which not only make it possible to interpret the numerical output but also provide an effective means of presenting the results to any audience. We have prepared a video for use at meetings (Matthews 1993, 1994; Matthews *et al.* 1994; Weiss 1994) but we shall rely here on monochromatic images that have been carefully selected.

The paper is organized as follows. The governing equations are introduced in the next section, together with the geometry, boundary conditions and parameters that define our model problem. The numerical methods are discussed in §3. Results obtained with a diffusivity ratio $\zeta = 1$, so that the initial bifurcation leads to steady convection, are presented in §4. Here we describe the competition between rolls and squares (in cells with a square planform) and that between rolls and hexagons (in rectangular cells), together with two- and three-dimensional streaming instabilities and different types of pulsating wave. Next, in §5, we give results for $\zeta = 0.1$, so that oscillatory behaviour appears at onset. Here we find both two-dimensional travelling rolls and three-dimensional alternating rolls in the nonlinear regime. In the final section we discuss the implications of these results and their relation to parallel investigations, and we conclude by indicating directions for future work.

2. Equations for compressible magnetoconvection

Our mathematical model for compressible magnetoconvection consists of a horizontal layer of compressible fluid permeated by a vertical magnetic field. We assume that the heat capacities c_p and c_v, the thermal conductivity K, the viscosity μ, the magnetic diffusivity η, the permeability μ_0 and the acceleration due to gravity g are all constant. The model is identical to that used in the two-dimensional calculations of Hurlburt *et al.* (1989).

Dimensionless variables are introduced by scaling length with the depth of the layer d, temperature with the fixed temperature T_0 at the upper surface, density with the density ρ_0 at the upper surface in the absence of convection, and magnetic field with the strength of the initial vertical magnetic field, B_0. For the time unit we use the isothermal sound travel time at the top of the layer, $d/(R_* T_0)^{1/2}$ where $R_* = c_p - c_v$ is the gas constant; this is equivalent to scaling the pressure to be unity at the top of the layer in the static state. This scaling for time is slightly different from that used by Hurlburt *et al.* (1989).

This non-dimensionalization introduces a number of dimensionless parameters to the problem. These are: the Prandtl number, $\sigma = \mu c_p/K$; the ratio of magnetic

Symbol	Parameter	Values used
σ	Prandtl number	0.1
ζ	mid-layer magnetic diffusivity	0.1 and 1.0
m	polytropic index	0.25
θ	thermal stratification	6
γ	ratio of specific heats	5/3
κ	dimensionless conductivity	variable
F, β	dimensionless field strength	variable
R	Rayleigh number	variable
Q	Chandrasekhar number	variable
λ_x	length of box in x-direction	variable
λ_y	length of box in y-direction	variable

TABLE 1. Parameters for the problem and values used in the computations

to thermal diffusivity at the top of the layer, $\zeta_0 = \eta c_p \rho_0 / K$; the polytropic index, $m = gd/R_* \Delta T - 1$ where ΔT is the temperature difference between the top and bottom of the layer; the dimensionless temperature difference $\theta = \Delta T / T_0$; the ratio of specific heats $\gamma = c_p/c_v$; the dimensionless thermal diffusivity $\kappa = K/d\rho_0 c_p (R_* T_0)^{1/2}$; and the dimensionless field strength $F = B_0^2/R_* T_0 \rho_0 \mu_0$, which is twice the ratio of the magnetic pressure to the gas pressure at the top of the layer.

A number of secondary parameters can be derived from the seven dimensionless numbers above. The Chandrasekhar number, relating the strength of the magnetic field to diffusion, is

$$Q = F/\zeta_0 \sigma \kappa^2, \tag{2.1}$$

and is independent of depth. The following quantities depend on depth, and for these we will use their mid-layer values. An alternative measure of the magnetic field strength is the 'plasma beta' β, the ratio of gas pressure to magnetic pressure,

$$\beta = \frac{2}{F}\left(1 + \frac{\theta}{2}\right)^{m+1}. \tag{2.2}$$

The Rayleigh number, representing the ratio of the destabilizing superadiabatic temperature gradient to the stabilizing effects of thermal and viscous diffusion is

$$R = \frac{(m+1)\theta^2}{\sigma \kappa^2 \gamma}(m + 1 - m\gamma)(1 + \theta/2)^{2m-1}. \tag{2.3}$$

Since the ratio of magnetic to thermal diffusivity is also a function of z, it is convenient to define a mid-layer value, $\zeta = \zeta_0(1 + \theta/2)^m$.

We choose axes (x, y, z) so that the z-axis points vertically downwards. The lengths of the periodic box in the x- and y-directions are denoted by λ_x and λ_y. The primary and secondary parameters, and the values used in the computations are given in table 1.

The equation for conservation of mass is

$$\frac{\partial \rho}{\partial t} = -\nabla \cdot (\rho \boldsymbol{u}) \tag{2.4}$$

where ρ is the fluid density and $\boldsymbol{u}$ is the fluid velocity. The momentum equation is

$$\frac{\partial}{\partial t}(\rho \boldsymbol{u}) = -\nabla(P + FB^2/2) + \nabla \cdot (F\boldsymbol{BB} - \rho \boldsymbol{uu} + \sigma\kappa\tau) + \theta(m+1)\rho\hat{\boldsymbol{z}} \tag{2.5}$$

where $\boldsymbol{B}$ is the magnetic field, P is the pressure and τ is the stress tensor,

$$\tau_{ij} = \frac{\partial u_i}{\partial x_j} + \frac{\partial u_j}{\partial x_i} - \frac{2}{3}\delta_{ij}\frac{\partial u_k}{\partial x_k}. \tag{2.6}$$

The induction equation is

$$\frac{\partial \boldsymbol{B}}{\partial t} = \nabla \times (\boldsymbol{u} \times \boldsymbol{B} - \zeta_0 \kappa \nabla \times \boldsymbol{B}) \tag{2.7}$$

and the heat equation is

$$\frac{\partial T}{\partial t} = -\boldsymbol{u} \cdot \nabla T - (\gamma - 1) T \nabla \cdot \boldsymbol{u} + \frac{\gamma \kappa}{\rho}\nabla^2 T + \frac{\kappa(\gamma - 1)}{\rho}(\sigma \tau^2/2 + F\zeta_0 J^2) \tag{2.8}$$

where T is the temperature and $\boldsymbol{J} = \nabla \times \boldsymbol{B}$. The terms in (2.8) represent temperature changes due to advection, compression, diffusion, viscous heating and Joule heating respectively. The pressure P is given by the equation of state

$$P = \rho T \tag{2.9}$$

and the magnetic field is solenoidal,

$$\nabla \cdot \boldsymbol{B} = 0. \tag{2.10}$$

This last condition, together with (2.7), implies that the magnetic flux through any horizontal surface, $\int B_z \, \mathrm{d}x \, \mathrm{d}y$, is independent of z and t.

We choose boundary conditions that are simple and consistent with previous work, rather than trying to construct more elaborate boundary conditions that might be more appropriate for the Sun. All variables are assumed to be periodic in the horizontal directions. The boundary conditions imposed at the upper and lower surfaces of the layer are that the normal velocity and horizontal shear stress are zero, that the temperature is fixed and that the magnetic field is vertical.

The equations (2.4)–(2.10) have a stationary polytropic solution in which $\boldsymbol{u} = 0$, $\boldsymbol{B} = \hat{\boldsymbol{z}}$, $T = 1 + \theta z$, $\rho = (1 + \theta z)^m$ and $P = (1 + \theta z)^{m+1}$. This state was used as the initial condition, with a small random perturbation added to the temperature field.

The Boussinesq equations can be obtained from the fully compressible equations (2.4)–(2.10) by taking the limit $\theta \to 0$ with $F \sim \theta^2$, $\kappa \sim \theta$. In this limit the rate of change of convective modes scales with θ while the sound speed remains of order 1. Thus it is numerically difficult to approach the Boussinesq limit since for small θ most of the computational effort is expended on tracking sound waves while the convective modes evolve slowly.

We end this section with a brief summary of linear stability theory. Further details can be found in Hurlburt *et al.* (1989). The magnetic diffusivity ratio ζ is particularly important. If ζ is small, the magnetic field is wound up by the convection, and the resulting Lorentz force becomes large enough to reverse the motion. This leads to oscillatory convection, provided that the magnetic field strength is sufficiently large. If ζ is large, the magnetic field can 'slip' through the fluid, allowing convection to be steady. In both the steady and oscillatory cases, increasing the magnetic field strength has three effects: (*a*) the magnetic field resists convection, so a larger Rayleigh number is required before convection occurs, and beyond a certain field strength convection will not occur for any Rayleigh number; (*b*) the preferred width of convection rolls narrows; (*c*) the increasing magnetic pressure leads to greater fluctuations in density and hence a greater departure from the Boussinesq approximation.

3. Numerical methods

The equations are solved by an extension and modification of the mixed finite-difference/pseudospectral code of Cattaneo *et al.* (1991) for compressible convection with no magnetic field. Differentiation is carried out by a spectral method using fast Fourier transforms in the periodic x- and y-directions. Spectral methods are very much more accurate than finite-difference methods for problems with periodic boundary conditions when the solutions are smooth (Canuto *et al.* 1988). Close to the onset of convection, it is known that the behaviour is governed by a small number of Fourier modes in the horizontal directions. In the vertical direction, the code uses an explicit fourth-order finite-difference method.

The equations for conservation of mass, momentum and magnetic field are written in conservative form, ensuring that mass, momentum, the average vertical component of the magnetic field and the divergence of the magnetic field are conserved to machine precision.

The time integration uses the explicit, second-order Adams–Bashforth method. The choice of time-step is restricted by stability constraints relating to the diffusion time and the wave travel time over a mesh interval. These two limits were found to be similar in magnitude.

For the mildly nonlinear convection in the range explored in this paper, a fairly low resolution is sufficient. Most of the results were obtained using 16 points (8 complex Fourier modes) in the x- and y-directions, and 25 points in the z-direction. Higher resolution was used in the z-direction because the finite-difference method is less accurate than the spectral method. To test the accuracy of the discretization, a number of runs were carried out with only 12 points in the x- and y-directions, and 17 points in the z-direction. These were found to agree with the higher-resolution results to within about 5%. The code was also checked against the two-dimensional results of Hurlburt *et al.* (1989).

The calculations were carried out using Sun and HP workstations and the Convex supercomputer at ULCC.

4. Steady magnetoconvection and secondary bifurcations ($\zeta = 1$)

We now describe in detail the results of our numerical simulations. In order to focus attention on the magnetic field, and for the purposes of comparison with earlier work, the parameters governing the polytropic atmosphere were fixed at $\gamma = 5/3$, $m = 1/4$, $\theta = 6$. This means that while the temperature increases by a factor of 7 across the layer and the pressure contrast is 11.4, the density contrast is only 1.63. The choice of $m = 1/4$ gives a temperature gradient that is twice the adiabatic temperature gradient. The Prandtl number σ was fixed at 0.1. These parameters are the same as those used by Hurlburt *et al.* (1989) and Proctor *et al.* (1994) in their two-dimensional calculations. The other parameters of the problem, including the Rayleigh number R, the ratio of gas pressure to magnetic pressure β and the magnetic diffusivity ratio ζ were allowed to vary in order to explore several different regimes of magnetoconvection.

Our results are divided into four sections. Steady convection is investigated by setting $\zeta = 1$. We first set $\lambda_x = \lambda_y$, allowing a planform of rolls or squares. In §4.1 the weak field case is explored, where we find that rolls are preferred at onset but become unstable to a streaming instability. In the strong field regime (§4.2) squares are stable. To allow a hexagonal planform, a rectangular geometry with $\lambda_x = \sqrt{3}\,\lambda_y$

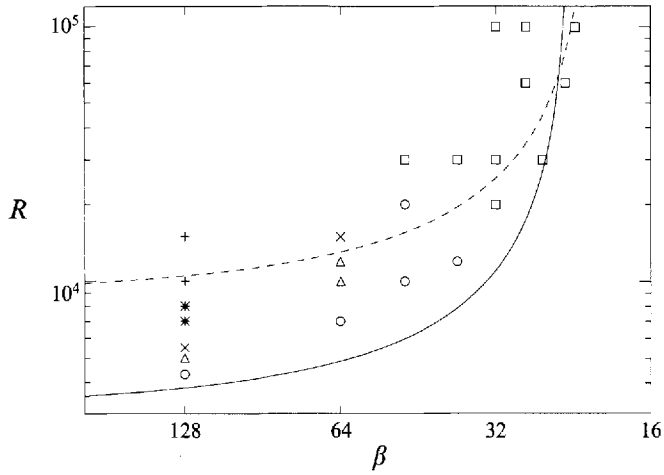

FIGURE 1. Steady magnetoconvection, $\zeta = 1.0$. Circles – stable rolls, triangles – rolls plus steady shear flow, crosses – rolls plus periodic shear flow, asterisks – pulsating waves, plus signs – alternating pulsating waves, squares – squares. The solid and dashed lines are the linear stability boundaries for wavenumbers $k = 2\pi$ and $k = 2\sqrt{2}\pi$.

is considered in §4.3. Oscillatory convection is studied by setting $\zeta = 0.1$, in §5. In the oscillatory case, we restrict attention to the case $\lambda_x = \lambda_y$.

4.1. *Weak fields with $\lambda_x = \lambda_y$: rolls and their instabilities*

To interpret the results it is important to consider which wavenumbers can occur in the periodic box. For two-dimensional convection in a periodic box of length λ_x, the possible wavenumbers are simply $2n\pi/\lambda_x$. In three dimensions however, rolls need not be aligned with the axes, and the possible wavenumbers in a square box ($\lambda_x = \lambda_y$) are $2\pi(n^2 + m^2)^{1/2}/\lambda_x$ for any integers n, m, corresponding to a planform with horizontal dependence $\sin\big((nx + my)2\pi/\lambda_x\big)$. For example, if $\lambda_x = \lambda_y = 1$, rolls with wavenumber 2π aligned with the axes or rolls with wavenumber $2\sqrt{2}\pi$ aligned diagonally are both allowed.

Figure 1 shows the linear stability curves for the onset of steady convection as a function of the Rayleigh number R and the field strength parameter β, for wavenumbers $k = 2\pi$ and $k = 2\sqrt{2}\pi$. These results were obtained using the linear code of Cattaneo (1984), and several points on the curves were checked using a two-dimensional version of the fully nonlinear code. The Rayleigh number is varied by adjusting the dimensionless diffusivity κ. Therefore the vertical coordinate in figure 1 should be thought of as an inverse measure of the diffusion coefficients in the momentum, induction and heat equations, not as a measure of the temperature gradient.

Two regimes are clearly apparent in figure 1. When the field is weak, convection is resisted by thermal and viscous diffusion and the magnetic field is essentially passive. For stronger fields, convection is resisted by the magnetic field, and for each wavenumber there is a critical field strength beyond which convection cannot occur for any Rayleigh number. In this second region, convection occurs in narrower cells. This is apparent from the crossing of the linear stability curves in figure 1. As the diffusion coefficients are decreased, so that R and Q increase, the preferred wavenumber increases but the maximum field strength does not increase significantly.

λ_x	β	R	Result
1.0	128	4300	2D rolls
1.0	128	5000	2D rolls + steady shear flow
1.0	128	5500	2D rolls + periodic shear flow
1.0	128	7000	2D pulsating wave
1.0	128	10000	3D alternating pulsating wave
1.0	64	7000	2D rolls
1.0	64	10000	2D rolls + steady shear flow
1.0	64	15000	2D rolls + periodic shear flow
1.0	48	10000	2D rolls
1.0	48	20000	2D rolls
1.0	48	30000	3D squares at top, rolls at bottom
1.0	38	12000	2D rolls
1.0	32	20000	3D squares
1.0	32	30000	3D squares
1.0	26	30000	3D squares
1.0	28	60000	3D squares
1.0	23.5	60000	3D subcritical squares
1.0	28	100000	3D squares
1.0	23	100000	3D subcritical squares
2.0	128	2000	2D rolls
2.0	128	2500	2D rolls + steady shear flow
2.0	56	3700	3D squares

TABLE 2. Summary of runs for steady convection with $\lambda_x = \lambda_y$. Note that the results for the two different aspect ratios are not directly comparable, as the critical Rayleigh numbers are different (cf. figure 1)

For weak fields, convection with a wavenumber of 2π is preferred over convection with a wavenumber of $2\sqrt{2}\pi$, but for stronger fields convection with the larger wavenumber is preferred. Thus if we fix $\lambda_x = 1$, a change of scale will occur as the field strength is increased, from convection cells with wavenumber 2π aligned with the box, to cells with wavenumber $2\sqrt{2}\pi$ aligned diagonally with the box.

Most runs were carried out with $\lambda_x = 1$, so that the box is a cube and the convection cells are twice as tall as they are wide. This is appropriate for convection in a strong field, but forces the cells to be narrower than their preferred wavelength when the field is weak. To check whether this has any qualitative influence on the behaviour, a few runs were carried out with $\lambda_x = 2$ for large values of β. Table 2 summarizes the results of the calculations for steady magnetoconvection with $\zeta = 1$ and $\lambda_x = \lambda_y$. The results with $\lambda_x = \lambda_y = 1$ are shown in figure 1.

For $\lambda_x = \lambda_y = 1$ and $\beta = 128$ the critical Rayleigh number is 3790. As the Rayleigh number is increased, the following behaviour is observed. At $R = 4300$, convection takes the form of steady, symmetric two-dimensional rolls. A symmetry-breaking pitchfork bifurcation then occurs, and at $R = 5000$ convection takes the form of a slowly travelling wave with a steady, mean shear flow. This behaviour is shown in figure 2; the shear flow leads to tilted cells, and enhances the cell that has a vorticity in the same sense as the shear flow. To quantify the shear flow we use the ratio of the mean flow at the top of the layer to the r.m.s. velocity; this ratio has the value 0.17 for the solution shown in figure 2.

This instability to a mean shear flow has been analysed for the non-magnetic case by Howard & Krishnamurti (1986) and Prat, Massaguer & Mercader (1995), for a

FIGURE 2. Instability of two-dimensional rolls to steady shear flow. The arrows show instantaneous streamlines and the shading is proportional to the density. There is a net shear flow to the right at the top of the layer and to the left at the bottom, giving rise to a travelling wave that drifts to the right at speed $v = 0.019$. The maximum value of the horizontal velocity is 0.42, and the mean flow has a maximum of 0.11. Parameters are $\zeta = 1$, $\beta = 128$, $R = 5000$.

vertical magnetic field by Proctor *et al.* (1994) and Matthews *et al.* (1993), and for a horizontal field by Lantz (1995). Physically, convection rolls can be unstable to a shear flow because the shear flow causes the rolls to tilt, while tilted rolls transport horizontal momentum to the top and bottom of the layer in such a way as to enhance the shear flow.

At $R = 5500$, the system has undergone a Hopf bifurcation to modulated waves, and makes an oscillation about the sheared state. The ratio of mean flow to r.m.s. flow varies between 0.06 and 0.36 during the oscillation. As R increases, this oscillation increases in amplitude, and when $R = 7000$, it has collided (along with its mirror image) with the steady untilted roll solution at a global bifurcation, creating a large-amplitude oscillation in which the direction of the shear flow reverses periodically. The maximum mean flow ratio is now 0.63. Further details of this 'gluing' bifurcation can be found in Rucklidge & Matthews (1995*a*). This two-dimensional behaviour is referred to as a pulsating wave; it has symmetry under a reflection in a vertical plane and an advance of half a period in time. Pulsating waves and the bifurcations which lead to their formation are described in more detail by Matthews *et al.* (1993) and Proctor *et al.* (1994); the sequence of bifurcations found in the numerical experiments can be reproduced in a fifth-order truncated model. The pitchfork and Hopf bifurcations are found also in Bénard convection (Howard & Krishnamurti 1986). The global bifurcation, which may be homoclinic or heteroclinic, is extremely complicated (Rucklidge & Matthews 1995*a*), and may or may not lead to a pulsating wave. The presence of a magnetic field facilitates reversals in the shear flow, since the shear flow stretches out the magnetic field leading to a strong restoring force.

When R is increased to 10000, the behaviour becomes three-dimensional and a more complicated sequence occurs. The initial behaviour is the same as at $R = 7000$, with steady two-dimensional convection in the x-direction becoming unstable to a pulsating wave in which the shear flow reverses direction. The shear flow is now more vigorous (the maximum ratio of shear flow to r.m.s. velocity is now 0.90) and is very effective at suppressing convection in the x-direction. However, convection in the y-direction is not affected by the shear flow. This allows convection in the y-direction to grow exponentially, and after several complete cycles of the oscillation, convection in the y-direction takes over. These y-rolls then become unstable to the shearing instability and the above sequence is repeated. This novel consequence of the shear flow instability, whereby the mean flow suppresses the rolls and leads to orthogonal rolls, was not found in earlier studies of the instability, which have restricted attention to two dimensions. We will refer to this new behaviour as an 'alternating pulsating wave'. We note that the mechanism for its generation described above does not depend on the magnetic field or the compressibility of the layer; therefore we expect that alternating pulsating waves may also be found in Rayleigh–Bénard convection (Matthews *et al.* 1996).

A clearer form of alternating pulsating wave was found near the branch of unstable steady solutions which exists with $\zeta = 0.1$ for weak fields, and this solution is shown in figure 3. With $\beta = 1024$ and $R = 6000 = 1.5R_c$, symmetric convection in the x-direction (figure 3*a*) becomes unstable to a shear flow (figure 3*b*). This shear flow suppresses convection and decays, allowing convection in the y-direction to grow (figure 3*c*,*d*). This in turn becomes unstable to a shear flow in the y-direction, and so on, so the behaviour is periodic and figure 3 shows 1/4 of the complete cycle. The periodic solution has a symmetry under rotation through 90° and an advance of 1/4 of a time period. This run was carried out as a three-dimensional extension of the case studied by Proctor *et al.* (1994). Further details of the dynamics associated with this shearing instability in two and three dimensions will be discussed in a future work (Rucklidge & Matthews 1995*b*).

To investigate whether the appearance of this shearing instability is enhanced by the fact that we are choosing λ_x to be smaller than the preferred cell width, some runs were carried out with $\lambda_x = \lambda_y = 2.0$. For $\beta = 128$ the critical Rayleigh number is 1210 (instead of 3790). Steady rolls were found to be stable at $R = 2000$; however, a steady shear flow was found at $R = 2500$ (instead of 5000). The ratio of the shear flow to the r.m.s. flow is 0.51 in this case. With $\lambda_x = \lambda_y = 4.0$, $\beta = 128$ and $R = 2500$, the shear flow oscillates, without reversing, and the maximum ratio is 0.42. Therefore we can conclude that the occurrence of the shear flow instability is not an artefact of the narrow boxes used in the runs described above.

4.2. *Strong fields: squares and* $\sqrt{2}$: 1 *resonance*

For stronger magnetic fields, squares were found to be stable (see figure 1 and table 2); squares were found to be preferred to rolls for all field strengths greater than $\beta = 32$. Unlike squares normally found in Boussinesq convection problems, these squares have an up-down asymmetry and a 'hexagon-like' topological structure: the rising fluid is confined to an isolated plume, and the downflow occurs in sheets around the edges of the cell. The velocity and density for this asymmetric square solution are shown in figure 4. Similar asymmetric squares have been observed in convection experiments using syrup with a temperature-dependent viscosity (White 1988).

This behaviour can be understood by the use of a low-order model. The predominant Fourier modes of these squares suggest that their horizontal dependence can

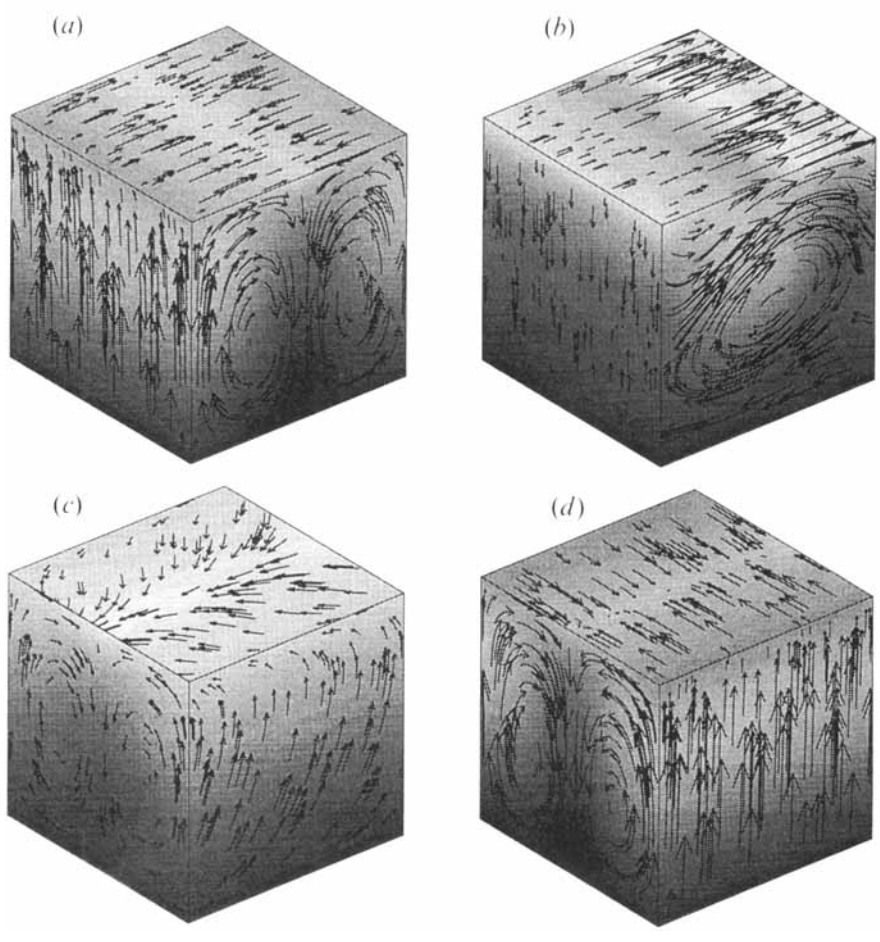

FIGURE 3. An alternating pulsating wave, $\zeta = 0.1$, $R = 6000$, $\beta = 1024$. Shading is proportional to density and the arrows indicate the direction and magnitude of the flow. The frames show 1/4 of the complete cycle and are separated by 1/12 of the period.

be described by the planform function $h(x, y) = A\cos kx + B\cos ky + C\cos kx\cos ky$, with $A = B$. Convection of this form was first proposed by Drobyshevski & Yuferev (1974) in the context of topological pumping of magnetic fields. This form of convection arises naturally from a resonance between modes A and B with wavenumber k, aligned with the box, and mode C with wavenumber $k\sqrt{2}$. In the neighbourhood of the point where the two linear stability curves in figure 1 cross, these are the dominant modes and they have similar growth rates. A full analysis of this $\sqrt{2} : 1$ resonance will be presented in a future paper (Proctor & Matthews 1996), and has some similarities with the $2 : 1$ resonance studied by Jones & Proctor (1987). This analysis involves four complex equations, but these equations have a third-order invariant subspace in the modes A, B and C, with the amplitude equations

$$\dot{A} = \mu A + \delta BC + \ldots, \tag{4.1}$$

$$\dot{B} = \mu B + \delta AC + \ldots, \tag{4.2}$$

$$\dot{C} = \nu C + \gamma AB + \ldots, \tag{4.3}$$

where the dots indicate terms of cubic or higher order. This subspace is attracting if

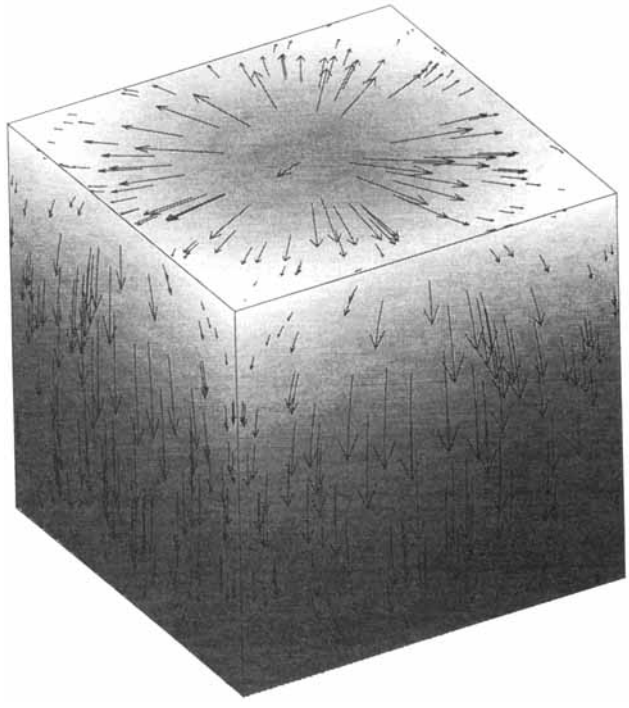

FIGURE 4. Steady squares, with $\beta = 28$, $R = 30000$.

$\delta\gamma > 0$. Here μ and ν are parameters related to R and β, while γ and δ are constants related to the up-down asymmetry of the layer. The quadratic resonant terms in these amplitude equations can only occur for a non-Boussinesq fluid, since in the Boussinesq case there is up-down symmetry which implies symmetry under a sign change of any mode. Analysis of (4.1)–(4.3) shows that if δ and γ have the same sign then rolls can become unstable and stable asymmetric squares (represented by a combination of A, B and C) can occur subcritically, i.e. when μ and ν are both negative. This latter possibility appears to be the case in our numerical simulations: for $R = 60000$ and for $R = 100000$, stable squares were found for subcritical values of β. In each case, the maximum value of β for which squares could be found was 3% below critical.

This preference for three-dimensional flow at the onset of convection is a consequence of the stratification of the layer. As the magnetic field strength is increased, progressively larger density fluctuations are induced by magnetic pressure. Thus the degree of departure from the Boussinesq approximation increases, and hence the resonant quadratic terms δ and γ in the amplitude equations (4.1)–(4.3) also increase. For Boussinesq magnetoconvection, rolls are always preferred over squares (Clune & Knobloch 1994). When the stratification of the layer was reduced by decreasing θ to 1 and raising β to 376, with $R = 20000$, it was found that rolls are stable at onset.

Near the boundary between the region of stable rolls and stable squares a mixed mode was found which has the form of squares at the top of the layer and rolls at the bottom. Figure 5 shows this solution, for $\beta = 48$, $R = 30000$. This mixed mode can also be found in the low-order model described above (Proctor & Matthews 1996). Physically, this behaviour can be understood in terms of stratification of the layer. At the bottom of the layer the pressure and sound speed are greater than at the top, so the fluid there is closer to the Boussinesq limit. By the argument in the previous

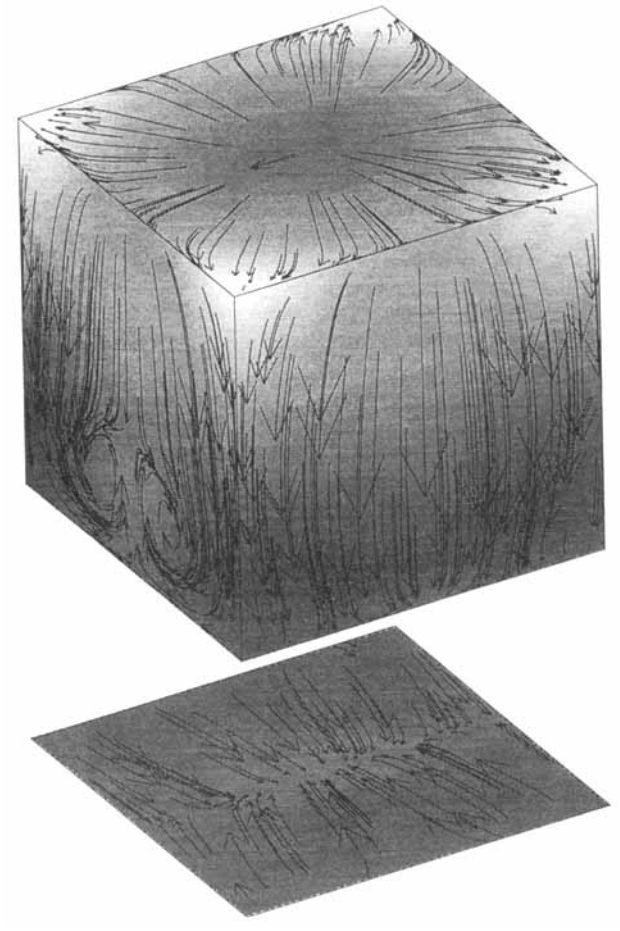

FIGURE 5. A steady solution with a square pattern at the top of the layer and rolls at the bottom. Parameters are $\beta = 48$, $R = 30000$.

paragraph, a solution with rolls at the bottom of the layer and squares at the top might be expected.

Squares can also become unstable to a weak form of the shear flow instability described in §4.1 above. For $\beta = 38$ and $R = 30000$, a weak oscillatory shear flow occurs, leading to square cells with a slight tilt. This shear flow is aligned with the box, and the ratio of the mean flow to the r.m.s. flow has a maximum value of 0.05. Increasing the Rayleigh number to 40000 gives a steady shear flow of similar magnitude but aligned diagonally to the box. Note that this shear flow is much weaker than that found for rolls, so it only produces a small perturbation to the square planform. The resulting pattern travels slowly in the direction of the shear flow at the top of the layer.

The same transition from rolls to squares as the magnetic field strength is increased was observed for the wider aspect ratio, $\lambda_x = \lambda_y = 2$. For $\beta = 128$ and $R = 2000$, rolls are stable, but for $\beta = 56$ and $R = 4000$, stable squares were found, with the same topological structure as described above.

It cannot be denied that the observed planforms are strongly influenced by the aspect ratio chosen. However we see no reason why stable squares should not persist

λ_x	β	R	Result
4.4	110	1920	rolls with oscillation
4.4	110	1575	rolls with oscillation
4.4	110	1382	rolls
4.4	110	1319	rolls
4.4	110	1281	rolls
2.0	34	20000	'up' hexagons with oscillation
2.0	30	20000	'up' hexagons

TABLE 3. Summary of runs for steady convection with $\lambda_x = \sqrt{3}\,\lambda_y$

even if the computational domain were very large. Indeed, White's (1988) experiments demonstrate the existence of stable asymmetric squares in boxes of large aspect ratio.

4.3. *Steady magnetoconvection with $\lambda_x = \sqrt{3}\,\lambda_y$: rolls and hexagons*

The hexagonal planform function can be written as

$$h(x,y) = \cos kx + \cos\frac{k}{2}(y\sqrt{3}-x) + \cos\frac{k}{2}(y\sqrt{3}+x) \tag{4.4}$$

$$= \cos kx + 2\cos\frac{k}{2}x\cos\frac{\sqrt{3}k}{2}y. \tag{4.5}$$

Hexagons can be thought of as three sets of rolls aligned at 60°, and hexagons with wavenumber k can be obtained in a rectangular box if we choose $\lambda_x = 4\pi/k$ and $\lambda_y = 4\pi/\sqrt{3}k$. However, this choice of λ_x and λ_y also allows rolls aligned in the x-direction with wavenumbers $k/2$, k and $3k/2$, and rolls aligned in the y-direction with wavenumbers $\sqrt{3}k/2$. In order to ensure that the preferred wavenumber is the wavenumber k which allows the hexagonal planform, the value of λ_x must be chosen with care. For a given value of the field strength β, k was chosen to minimize the critical Rayleigh number. This ensures that the nonlinear behaviour will be governed by modes with wavenumber k, allowing either the hexagonal or roll planforms. The results for this case are summarized in table 3.

For steady non-Boussinesq convection, in which there is no symmetry under reflection in $z = 1/2$, hexagons will always occur at onset (Golubitsky, Swift & Knobloch 1984). This is because of the asymmetry between 'up' hexagons (with the flow directed upwards at the centre of the hexagons and downward around the edges) and 'down' hexagons (with the flow reversed). Thus we have a transcritical bifurcation to hexagons, implying the existence of subcritical convection.

For a field strength $\beta = 110$, the appropriate value of λ_x is 4.4. The results show that rolls are preferred over hexagons at values of the Rayleigh number 1.02, 1.05, 1.1, 1.25 and 1.5 times critical. Thus although we know from the lack of up-down symmetry in the problem that hexagons must be preferred at onset, stability is transferred to rolls at very low amplitude. It can easily be shown from the relevant amplitude equations for the interaction of rolls and hexagons that if the degree of asymmetry in the problem is ϵ, and rolls are stable when $\epsilon = 0$, then the range of Rayleigh numbers for which hexagons are stable is of order ϵ^2. Thus it is not surprising that hexagons are not found when the magnetic field is weak, in which case the departure of the system from the Boussinesq case is small.

These rolls become unstable to the oscillatory instability (Busse 1972) as the Rayleigh number is increased. This instability gives the rolls a wavy appearance, and

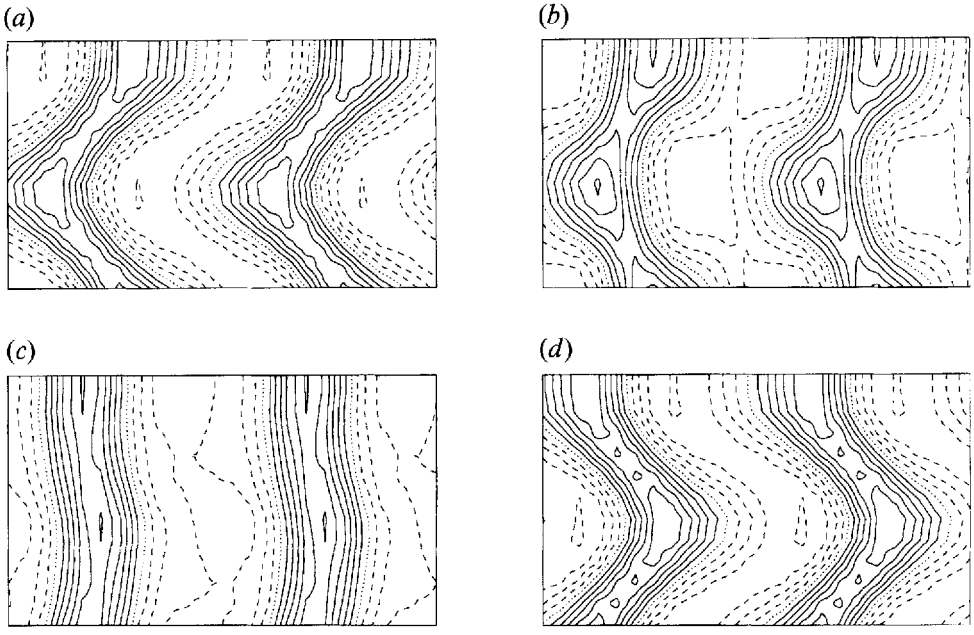

FIGURE 6. The oscillatory instability of rolls. Contours of the vertical velocity at the middle of the layer, at intervals of 2.5 time units. Solid (dashed) lines indicate descending (rising) fluid, and the parameter values are $\beta = 110$, $R = 1920$, $\lambda_x = 4.4$, $\lambda_y = \lambda_x/\sqrt{3}$.

is illustrated in figure 6 for $R = 1920 = 1.5R_c$. The period of the oscillation is 16.4 and the modulation here takes the form of a standing wave (though travelling waves may be possible for other aspect ratios). The oscillations involve the interaction of rolls with horizontal dependence $\cos kx$ and a mode proportional to $\sin kx \cos ky\sqrt{3}/2$. Since this instability is well known and does not depend on the magnetic field or the compressibility of the fluid, we do not investigate it further here. For $R = 1.25R_c$ the oscillations are smaller in amplitude, and for $R = 1.1R_c$ and $R = 1.05R_c$ the rolls are stable.

The strong-field regime was studied by fixing the Rayleigh number at $R = 20000$, for which the preferred wavelength for rolls is close to 1 and the critical value of β is 27.1. For $\beta = 30.2 = 1.1\beta_c$, stable hexagons were found. This solution is shown in figure 7: the individual plumes are almost circular but they lie on a hexagonal lattice. These are 'up' hexagons, i.e. they have the same topology as the squares described in §4.2, with isolated upflows and connected downflows. All of the hexagonal and square solutions we have found exhibit this topological structure, which seems to be a general feature of convection in a stratified fluid (Stein & Nordlund 1989; Cattaneo *et al.* 1991) and is consistent with the granulation pattern observed on the surface of the Sun. An obvious explanation of this effect is that in a stratified fluid a rising plume expands horizontally, while sinking plumes contract; a pattern of 'up' hexagons allows for horizontal expansion in isolated upflows near the top of the layer.

When the amplitude of convection is increased by reducing the field strength to $\beta = 34 = 1.2\beta_c$, these hexagons are modulated by a slow small-amplitude oscillation, of period 105. During this oscillation, the pattern changes from a regular hexagonal pattern to a more rectangular pattern. Figure 8 illustrates this behaviour, showing contours of the vertical velocity at the hexagonal and rectangular phases of the

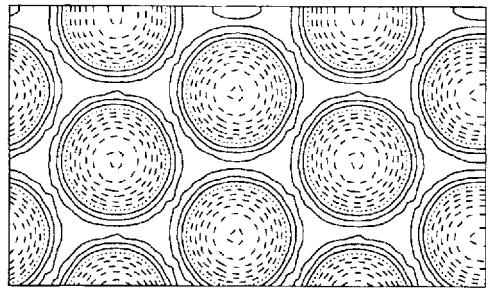

FIGURE 7. The steady hexagonal planform. Contours of the vertical velocity at the middle of the layer. Four of the computational boxes are shown in order to show the pattern more clearly. Parameter values are $\beta = 30$, $R = 20000$, $\lambda_x = 2$, $\lambda_y = \lambda_x/\sqrt{3}$.

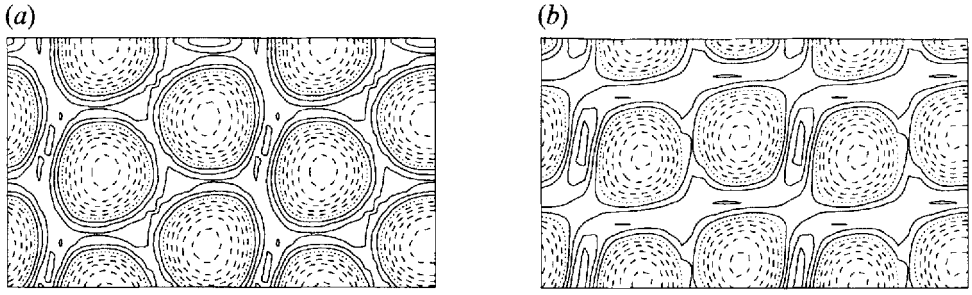

FIGURE 8. The oscillatory instability of hexagons at (*a*) the hexagonal and (*b*) the rectangular phase of the cycle. Contours of the vertical velocity at the middle of the layer. Four of the computational boxes are shown in order to show the pattern more clearly. Parameter values are $\beta = 34$, $R = 20000$, $\lambda_x = 2$, $\lambda_y = \lambda_x/\sqrt{3}$.

oscillation. This instability involves a mode of the form $\sin ky\sqrt{3}/2$, in the notation of (4.5).

5. Oscillatory magnetoconvection ($\zeta = 0.1$)

5.1. *Planforms for weakly nonlinear oscillatory convection with square symmetry*

In order to be able to interpret our numerical results in the oscillatory case, it is essential to understand the possible planforms that can occur at an oscillatory bifurcation. We restrict attention to planforms that are periodic on a square lattice, that is, those which can occur in our numerical experiments with a square box and periodic boundary conditions. The relevant planforms have been found by Swift (1988) for the case of interacting standing waves, and Silber & Knobloch (1991) for the more general case including travelling waves. The main results of these papers are summarized below.

At the onset of convection in a square box, the solution can be written as a combination of four travelling waves in the positive-x, negative-x, positive-y and negative-y directions. The horizontal dependence of any of the physical variables can be represented by a planform function

$$h(x,y) = \mathrm{Re}\left(x_+ e^{i(\omega t - kx)} + x_- e^{i(\omega t + kx)} + y_+ e^{i(\omega t - ky)} + y_- e^{i(\omega t + ky)}\right) \tag{5.1}$$

where k is the horizontal wavenumber, ω is the frequency associated with the Hopf bifurcation and x_+, x_-, y_+ and y_- are the complex amplitudes of the travelling waves.

The relevant amplitude equations for the evolution of the four modes can be written to third order in amplitude as

$$\left.\begin{aligned}
\dot{x}_+ &= x_+(\lambda - a|x_+|^2 - b|x_-|^2 - c(|y_+|^2 + |y_-|^2)) + d\bar{x}_-y_-y_+,\\
\dot{x}_- &= x_-(\lambda - a|x_-|^2 - b|x_+|^2 - c(|y_+|^2 + |y_-|^2)) + d\bar{x}_+y_-y_+,\\
\dot{y}_+ &= y_+(\lambda - a|y_+|^2 - b|y_-|^2 - c(|x_+|^2 + |x_-|^2)) + d\bar{y}_-x_-x_+,\\
\dot{y}_- &= y_-(\lambda - a|y_-|^2 - b|y_+|^2 - c(|x_+|^2 + |x_-|^2)) + d\bar{y}_+x_-x_+,
\end{aligned}\right\} \tag{5.2}$$

where λ, a, b, c and d are complex constants. These equations (5.2) can be derived without any knowledge of the governing partial differential equations. For example, for the equation for x_+, we simply seek combinations of the four travelling waves which are proportional to $e^{i(\omega t - kx)}$. The symmetry of the problem under reflection is used to show that the coefficients of the y_+ and y_- terms in the x_+ equation are equal, and the symmetry under rotation through $\pi/2$ can then be used to deduce the evolution equations for the other three waves. Note that the amplitude equations include a phase interaction, represented by the last term in (5.2).

The possible planforms are combinations of travelling waves or standing waves in the x- and y-directions, and can be found by seeking stationary solutions of (5.2). These are:

1. Travelling rolls: a travelling wave in one direction only, e.g. $x_+ \neq 0$, $x_- = y_+ = y_- = 0$.
2. Standing rolls: a standing wave in one direction only, e.g. $x_+ = x_- \neq 0$, $y_+ = y_- = 0$.
3. Travelling squares: travelling waves in both x- and y-directions, e.g. $x_+ = y_+ \neq 0$, $x_- = y_- = 0$.
4. Standing squares: standing waves in both directions, in phase, $x_+ = x_- = y_+ = y_- \neq 0$.
5. Alternating rolls: standing waves in both directions, out of phase, $x_+ = x_- = iy_+ = iy_- \neq 0$.

For certain parameter values, a combination of unequal standing waves exists, but this solution is always unstable. The stability of these solutions depends in a highly complicated way on the coefficients λ, a, b, c and d (Silber & Knobloch 1991). In some cases, more than one planform may be stable, while in others, no planform is stable even though all the bifurcations are supercritical. It is possible for convection to be quasi-periodic or even chaotic at onset, for certain parameter values, in which case solutions 2, 4 and 5 bifurcate supercritically but are unstable.

The coefficients λ, a, b, c and d can be found for oscillatory Boussinesq magnetoconvection by substituting the four linear travelling waves (5.1) into the Boussinesq equations and continuing a weakly nonlinear analysis up to third order in the amplitudes. This work has recently been done using computer algebra (Clune & Knobloch 1994), with the result that alternating rolls are found to be stable over a wide range of parameter values. The analogous calculation restricted to two dimensions, allowing only travelling rolls and standing rolls (equivalent to obtaining a and b in equations (5.2)), was carried out by Matthews & Rucklidge (1993), with the result that either travelling rolls or standing rolls can be stable, depending on the parameters.

5.2. *Numerical results for oscillatory magnetoconvection*

For oscillatory convection, the argument in favour of a hexagonal planform at onset no longer applies, since the oscillation removes the distinction between 'up' and 'down' hexagons. For simplicity we only consider the case $\lambda_x = \lambda_y$, allowing the five possible planforms for oscillatory convection with square symmetry discussed above. For most

λ_x	β	R	Result
1.0	110	8280	alternating rolls
1.0	32	7800	alternating rolls
1.0	32	9000	alternating rolls
1.0	11	10108	travelling rolls and alternating rolls
1.0	5.5	14388	travelling rolls and alternating rolls
1.0	5.5	19000	travelling rolls
1.0	4.5	30000	travelling rolls and alternating rolls, both with oscillation
1.0	4.2	30000	travelling rolls and alternating rolls
1.0	4.3	43200	travelling rolls and alternating rolls, both with oscillation
1.0	4.0	43200	travelling rolls and alternating rolls
2.0	110	2280	alternating rolls
2.0	32	2222	alternating rolls
2.0	32	3000	alternating rolls

TABLE 4. Summary of runs for oscillatory convection with $\lambda_x = \lambda_y$.

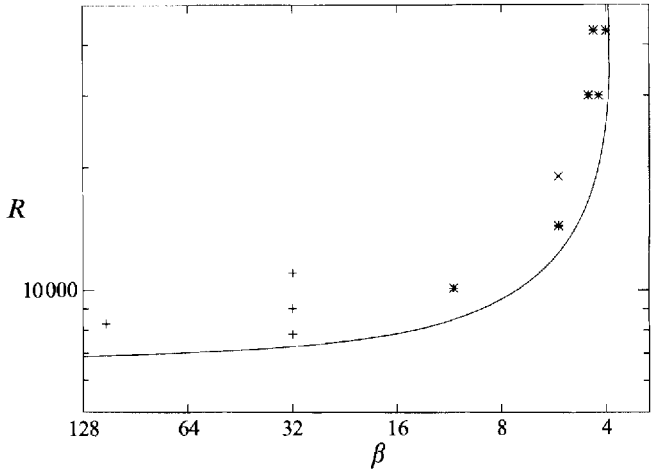

FIGURE 9. Oscillatory magnetoconvection, $\zeta = 0.1$. Plus signs indicate where alternating rolls are stable, crosses where travelling rolls are stable and asterisks where both patterns are stable. Both solutions are stable over a wide range of parameter values. The solid line is the linear stability boundary for $\lambda_x = 1$.

of our calculations, we choose a fixed box size $\lambda_x = \lambda_y = 1$. As in the steady case, this is appropriate for a relatively strong magnetic field, which leads to convection in narrow cells. For a weaker magnetic field the preferred cell width is wider, but we have checked that this does not qualitatively affect the preferred planform by doing a few runs with $\lambda_x = \lambda_y = 2$. Figure 9 shows the linear stability curve for the oscillatory case with $\lambda_x = 1$. As in the steady case, the two regimes where convection is limited predominantly by diffusion and by the magnetic field are clear. The results of the simulations are summarized in table 4 and figure 9.

For the case of a moderate magnetic field, the behaviour for convection restricted to two dimensions is a standing wave (Hurlburt *et al.* 1989). Our three-dimensional results show that for $\beta = 110$ and $\beta = 32$, the preferred planform near onset is the 'alternating rolls' pattern described above and by Silber & Knobloch (1991). The alternating roll planform can be thought of as a standing wave in the x-direction plus

a standing wave in the y-direction which is of the same amplitude but has a phase difference of $\pi/2$. The planform function, describing the horizontal dependence of the vertical velocity or the temperature, is proportional to $\cos kx \sin \omega t + \cos ky \cos \omega t$, and the horizontal velocity components u, v are proportional to $\sin kx \sin \omega t$ and $\sin ky \cos \omega t$ respectively. Thus the kinetic energy averaged over the layer is constant in time. The appearance of the convection pattern is of rolls aligned with the y-axis at $t = 0$, squares at a time $1/8$ of the period, and rolls aligned with the x-axis at $1/4$ of the period. The alternating rolls are symmetric under an advance of $1/4$ of a period in time and a rotation through 90° (note that this is the same symmetry as that of the alternating pulsating wave shown in figure 3). At a fixed point on the upper surface of the box, the velocity vector appears to rotate (in a clockwise or anti-clockwise direction depending on the point chosen). Thus Swift (1988) referred to this solution as a 'rotating wave'. Figure 10 shows the alternating roll solution at four stages in its cycle, for $\beta = 32$, $R = 7800$. The period of the oscillation in this case is 4.0. The qualitative behaviour when the box size is increased to $\lambda_x = \lambda_y = 2$ is the same: alternating rolls were found for $\beta = 110$ and $\beta = 32$.

This result that alternating rolls are stable over a wide range of parameter values is in qualitative agreement with the recent analytical work of Clune & Knobloch (1994), who used computer algebra to compute the coefficients of the weakly nonlinear amplitude equations (5.2) for Boussinesq magnetoconvection. Exact agreement is not to be expected, first because the weakly nonlinear analysis is only valid in a small region of parameter space, and secondly because our computations are non-Boussinesq.

The almost ubiquitous occurrence of alternating rolls may be explained by the following physical argument: overturning two-dimensional convection in, say, the (x, z)-plane winds up the magnetic field in that plane. The distorted magnetic field resists the motion, leading to oscillations in the form of a standing wave in the two-dimensional problem. In three dimensions, however, the distorted magnetic field provides less resistance to motion in the (y, z)-plane than to motion in the (x, z)-plane, so the fluid motions grow in the (y, z)-plane and decay in the (x, z)-plane. The field then becomes distorted in the (y, z)-plane and 'unwound' in the (x, z)-plane, so that motion then reverts to the (x, z)-plane.

For a stronger magnetic field, we find that more than one planform can be stable. For $\beta = 11$ with $R = 10108 = 1.2R_c$, alternating rolls were found when the usual procedure of starting the calculation from a small perturbation from the polytropic equilibrium was followed. However, when the system was started from an initial condition of a travelling wave, this state was found to be stable to three-dimensional disturbances. The travelling wave was obtained by using a two-dimensional version of the code; this was then used as an initial condition for the three-dimensional code, after the addition of a perturbation to the temperature field and the velocity field in the third direction. It was found that this three-dimensional perturbation decays exponentially.

At $\beta = 5.5$, and $R = 1.2R_c$, stable travelling rolls were found from the small-amplitude initial condition. When the system was started from the alternating roll solution obtained from $\beta = 11$, this was also found to be stable. In this case, the exponential decay of the disturbance was measured by the degree of left-right asymmetry in the second and third Fourier modes of the vertical velocity.

This result that both alternating rolls and travelling rolls are stable for some parameter values is consistent with the bifurcation analysis of Silber & Knobloch (1991) and Clune & Knobloch (1994), and complicates the numerical procedure of

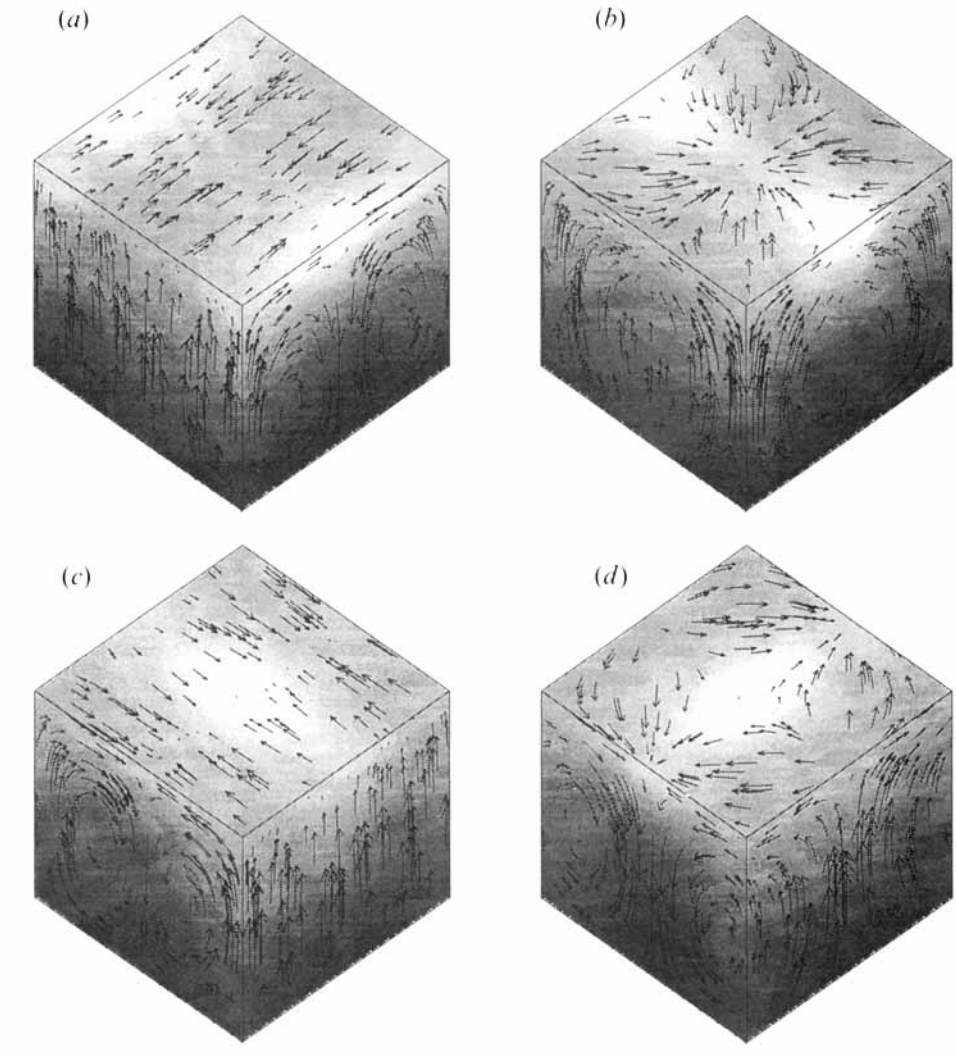

FIGURE 10. Alternating rolls, shown at intervals of 1/8 of the cycle. Arrows show velocity components in the plane of each of the three faces, and shading denotes density.

seeking solutions, since merely doing one run from a random initial condition does not completely describe the possible behaviour of the system.

The strong-field regime was studied by fixing the Rayleigh number and varying the field strength β. For both $R = 30000$ and $R = 43200$, the solution obtained from the small-amplitude initial condition was travelling rolls, although alternating rolls were also found to be stable. Both the travelling rolls and the alternating rolls were found to be unstable to a three-dimensional oscillation as the field strength was decreased. Travelling rolls are stable at $R = 43200$ and $\beta = 4$, but when β is raised to 4.3 the travelling rolls become unstable to an oscillatory transverse motion. Figure 11 shows contours of the vertical velocity during just under one half of this oscillation. The mode of instability has a horizontal dependence of $\cos kx \cos ky$, and the instability seems to take the form of a standing wave in the y-direction. The period of this modulation is 92, much greater than the period of the travelling waves themselves

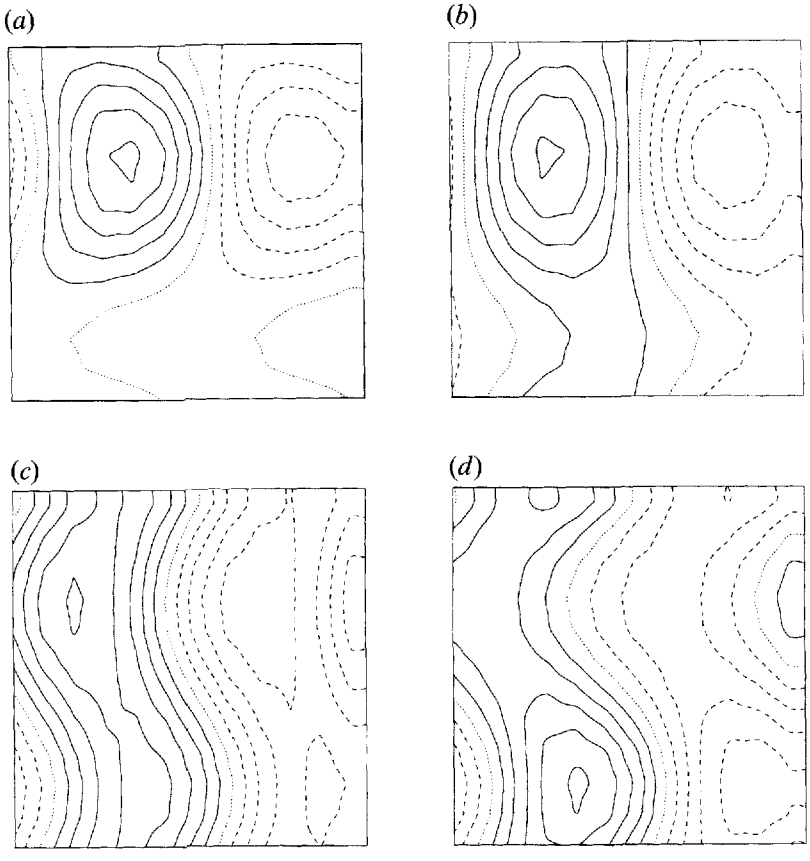

FIGURE 11. Modulated travelling rolls. Contours of the vertical velocity at the middle of the layer, at intervals of 11.0 time units. Solid (dashed) lines indicate descending (rising) fluid, and the parameter values are $\beta = 4.3$, $R = 43200$, $\lambda_x = \lambda_y = 1$.

which is only 2.2. The period of the instability decreases as its amplitude increases, suggesting that the bifurcation may be of pitchfork type.

When the field strength and the Rayleigh number are increased still further, the preferred mode for convection switches to rolls aligned diagonally with respect to the box, with a wavenumber greater by a factor of $\sqrt{2}$ than that of the rolls aligned with the box. Unlike the steady case discussed in §4.2 however, there are no quadratic resonant terms, because in the oscillatory case the two linear modes have different frequencies.

6. Conclusions and discussion

We have carried out a thorough investigation of preferred planforms for mildly nonlinear compressible convection in a vertical magnetic field, over a wide range of parameter values. The most striking and significant feature of our results is the range of ordered patterns for steady and, especially, time-dependent motion. When convection is steady and the field is weak, a planform of two-dimensional rolls is preferred over squares or hexagons. These rolls can be susceptible to a shear flow instability, which can in turn lead to three-dimensional flow, since the shear flow suppresses the convective velocity in its own plane but does not affect the orthogonal

rolls. In a stronger magnetic field, the non-Boussinesq density fluctuations are greater, leading to a preference for three-dimensional convection at onset. This flow takes the form of isolated upflows and connected downflows, and occurs with a planform of squares or hexagons, depending on the aspect ratio chosen for the box. An interesting question, hard to tackle numerically or analytically, is which of squares and hexagons would be preferred in an infinite layer. In the case of small ζ, when magnetoconvection is oscillatory, we find three-dimensional flow in the form of alternating rolls in the weak-field regime, while for stronger fields both alternating rolls and two-dimensional travelling rolls are stable at the same parameter values. Each of these solutions becomes unstable as the amplitude of convection is increased.

The interpretation of these results relies heavily on low-order models. Planform selection can be described by evolution equations with appropriate symmetries, and the preference for three-dimensional convection in a strong magnetic field, which does not occur in the Boussinesq approximation, is a consequence of compressibility, which leads to resonant terms in the amplitude equations for a stratified layer. When convection sets in at a Hopf bifurcation, our results can be compared with the amplitude equations derived by Clune & Knobloch (1994). Exact agreement is not to be expected, since they calculated the coefficients for incompressible flow. Nevertheless, there is considerable qualitative agreement; both studies show stable alternating rolls over a wide range of parameter values. Several questions requiring further work can be proposed. For instance, the complicated global bifurcations that lead to the appearance of two- and three-dimensional pulsating waves are being analysed by Rucklidge & Matthews (1995*a*, *b*). In the oscillatory case, a transition to steady convection occurs as the magnetic field strength is decreased. There is a codimension-two point at which the linear problem has two zero eigenvalues, where the steady and oscillatory branches meet. In two dimensions, the sequence of bifurcations leading from standing waves to steady convection is described by the Takens–Bogdanov normal form equations, and is well understood (e.g. Proctor & Weiss 1982; Dangelmayr & Knobloch 1987). In three dimensions, the relevant transition is from alternating rolls to steady rolls, and the bifurcation sequence remains to be explored.

The ordered patterns of behaviour that occur in the mildly nonlinear regime give way to chaos as the thermal forcing is increased. As might be expected, this transition occurs much earlier for three-dimensional convection than it does when the velocity and magnetic field are constrained to be two-dimensional. The natural extension of our work is to continue to larger Rayleigh numbers and to study the structure of chaotic magnetoconvection. To demonstrate what happens, we show here two examples of spatiotemporal chaos, or weak turbulence (Manneville 1991), in magnetoconvection at a Rayleigh number of 10000, with $\zeta = 0.1$ and $\lambda_x = \lambda_y = 2$, with $\beta = 113$ and $\beta = 23$ (figure 12). The nature of this highly complicated time-dependent convection is best appreciated on a video, from which it is clear that these solutions retain some of the character of alternating rolls, with rapid changes in the direction of the flow which compress the magnetic field into sheets and tubes alternately.

Of particular interest is the question of the spatial structure of a turbulent magnetic field. Does it essentially fill the whole space, as argued by Vainshtein *et al.* (1993), or does it form isolated magnetic structures in the form of flux sheets or tubes as found by Nordlund *et al.* (1994)? A satisfactory answer to this important and controversial question will not be reached until computing power increases to the point where a large number of simulations can be carried out at high resolution.

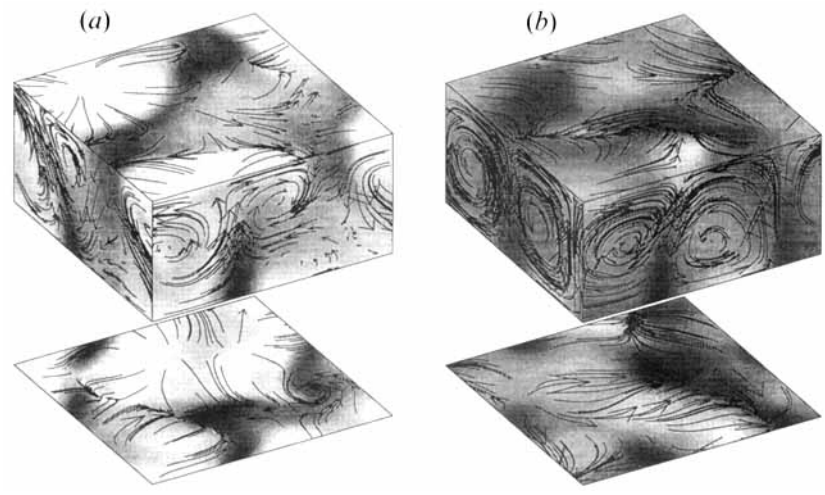

FIGURE 12. Aperiodic magnetoconvection (*a*) at $\beta = 113$, $R = 10000$ and (*b*) at $\beta = 23$, $R = 10000$. The shading indicates the magnitude of the magnetic field strength.

So far we have only considered a shallow stratified layer with an imposed field that is vertical. This configuration is too simple to explain behaviour in a sunspot. We are currently extending this work in order to investigate magnetoconvection in more strongly stratified layers, which model more closely the structure of a sunspot umbra. The stratification introduces new physical effects; convection may be oscillatory at the top of the layer and steady at the bottom due to the variation of ζ with depth (Weiss *et al.* 1990). Our preliminary results confirm that convection is three-dimensional in this case, as one might expect since increasing the stratification increases the asymmetry between the top and bottom of the layer and hence increases the preference for squares or hexagons, as discussed in §4.2.

The results of the present work are strongly influenced by our choice of a vertical magnetic field, which imposes square symmetry. Although the mean field is vertical at the centre of a sunspot, its inclination to the vertical increases to 45° at the edge of the umbra and to 70° at the outer boundary of the penumbra. We plan to study the case of an inclined field in three dimensions, extending the linear theory of Matthews *et al.* (1992) and the two-dimensional computations of Hurlburt, Matthews & Proctor (1995). We expect a transition from travelling rolls with axes normal to the plane of the inclined field to rolls with axes aligned with the field as the angle of inclination from the vertical is increased, but the manner of this transition is not clear. Sunspot penumbrae present a greater challenge. Their complicated filamentary structure is apparently associated with a new convective mode that carries heat inward from the surrounding plasma (Rucklidge, Schmidt & Weiss 1995). This process is intrinsically three-dimensional but it is not obvious how it can be modelled.

We are grateful to Fausto Cattaneo for generously letting us take over his hydrodynamic code and for advice on numerical methods, to Alastair Rucklidge for many enlightening comments and suggestions, and to Derek Brownjohn for producing some of the figures. We have also had helpful discussions with Neal Hurlburt, Edgar Knobloch, Mary Silber and Jim Swift. Financial support was provided by SERC and its successor PPARC, and supercomputer time by ULCC.

REFERENCES

BRANDENBURG, A., NORDLUND, A., PULKKINEN, P., STEIN, R. F. & TUOMINEN, I. 1990 3-D simulation of turbulent cyclonic magneto-convection. *Astron. Astrophys.* **232**, 277–291.

BROWNJOHN, D. P., HURLBURT, N. E., PROCTOR, M. R. E. & WEISS, N. O. 1995 Nonlinear compressible magnetoconvection. Part 3. Travelling waves in a horizontal field. *J. Fluid Mech.* **300**, 287–309.

BUSSE, F. 1972 The oscillatory instability of convection rolls in a low Prandtl number fluid. *J. Fluid Mech.* **52**, 97–112.

CANUTO, C., HUSSAINI, M. Y., QUARTERONI, A. & ZANG, T. A. 1988 *Spectral Methods in Fluid Dynamics*. Springer.

CATTANEO, F. 1984 Oscillatory convection in sunspots. In *The Hydromagnetics of the Sun* (ed. T. D. Guyenne), pp. 47–50. ESA SP 220.

CATTANEO, F., BRUMMELL, N. H., TOOMRE, J., MALAGOLI, A. & HURLBURT, N. E. 1991 Turbulent compressible convection. *Astrophys. J.* **370**, 282–294.

CHANDRASEKHAR, S. 1961 *Hydrodynamic and Hydromagnetic Stability*. Oxford University Press.

CLUNE, T. & KNOBLOCH, E. 1994 Pattern selection in three-dimensional magnetoconvection. *Physica* D **74**, 151–176.

DANGELMAYR, G. & KNOBLOCH, E. 1987 The Takens-Bogdanov bifurcation with $O(2)$ symmetry. *Phil. Trans. R. Soc. Lond.* A **322**, 243–279.

DROBYSHEVSKI, E. M. & YUFEREV, V. S. 1974 Topological pumping of magnetic flux by three-dimensional convection. *J. Fluid Mech.* **65**, 33–44.

GOLUBITSKY, M., SWIFT, J. W. & KNOBLOCH, E. 1984 Symmetries and pattern selection in Rayleigh-Bénard convection. *Physica* D **10**, 249–276.

HOWARD, L. N. & KRISHNAMURTI, R. 1986 Large-scale flow in turbulent convection: a mathematical model. *J. Fluid Mech.* **170**, 385–410.

HURLBURT, N. E., MATTHEWS, P. C. & PROCTOR, M. R. E. 1995 Nonlinear compressible convection in oblique magnetic fields. *Astrophys. J.*, in press.

HURLBURT, N. E., PROCTOR, M. R. E., WEISS, N. O. & BROWNJOHN, D. P. 1989 Nonlinear compressible magnetoconvection. Part 1. Travelling waves and oscillations. *J. Fluid Mech.* **207**, 587–628.

HURLBURT, N. E. & TOOMRE, J. 1988 Magnetic fields interacting with nonlinear compressible convection. *Astrophys. J.* **327**, 920–932.

JONES, C. A. & PROCTOR, M. R. E. 1987 Strong spatial resonance and travelling waves in Bénard convection. *Phys. Lett.* A **121**, 224–227.

KNOBLOCH, E., WEISS, N. O. & DA COSTA, L. N. 1981 Oscillatory and steady convection in a magnetic field. *J. Fluid Mech.* **113**, 153–186.

LANTZ, S. R. 1995 Magnetoconvection dynamics in a stratified layer. II. A low-order model of the tilting instability. *Astrophys. J.* **441**, 925–941.

MANNEVILLE, P. 1991 *Dissipative Structures and Weak Turbulence*. Academic Press.

MATTHEWS P. C. 1993 Compressible magnetoconvection in three dimensions. In *Solar and Planetary dynamos* (ed. M. R. E. Proctor, P. C. Matthews & A. M. Rucklidge), pp. 211–218. Cambridge University Press.

MATTHEWS P. C. 1994 Three-dimensional compressible magnetoconvection. In *Solar Active Region Evolution: Comparing Models with Observations* (ed. K. S. Balasubramaniam & G. W. Simon), pp. 56–61. Astron. Soc. Pacific.

MATTHEWS, P. C., HURLBURT, N. E., PROCTOR, M. R. E. & BROWNJOHN, D. P. 1992 Compressible magnetoconvection in oblique fields: linearized theory and simple nonlinear models. *J. Fluid Mech.* **240**, 559–569.

MATTHEWS, P. C., PROCTOR, M. R. E., RUCKLIDGE, A. M. & WEISS, N. O. 1993 Pulsating waves in nonlinear magnetoconvection. *Phys. Lett.* A **183**, 69–75.

MATTHEWS, P. C., PROCTOR, M. R. E., RUCKLIDGE, A. M. & WEISS, N. O. 1994 Nonlinear three-dimensional magnetoconvection in a compressible atmosphere. In *Solar Magnetic Fields* (ed. M. Schüssler & W. Schmidt), pp. 279–281. Cambridge University Press.

MATTHEWS, P. C. & RUCKLIDGE, A. M. 1993 Travelling and standing waves in magnetoconvection. *Proc. R. Soc. Lond.* A **441**, 649–658.

MATTHEWS, P. C., RUCKLIDGE, A. M., WEISS, N. O. & PROCTOR, M. R. E. 1996 The three-dimensional development of the shearing instability of convection. Submitted to *Phys. Fluids.*

NORDLUND, A., BRANDENBURG, A., JENNINGS, R. L., RIEUTORD, M., RUOKOLAINEN, J. & TUOMINEN, I. 1992 Dynamo action in stratified convection with overshoot. *Astrophys. J.* **392**, 647–652.

NORDLUND, A., GALSGAARD, K. & STEIN, R. F. 1994 Magnetoconvection and magnetoturbulence. In *Solar Surface Magnetism* (ed. R. J. Rutten & C. J. Schrijver), pp. 471–498. Kluwer.

NORDLUND, A. & STEIN, R. F. 1990 Solar magnetoconvection. In *Solar Photosphere: Structure, Convection and Magnetic Fields* (ed. J. O. Stenflo), pp. 191–211. Kluwer.

PRAT, J., MASSAGUER, J. M. & MERCADER, I. 1995 Large-scale flows and resonances in 2-D thermal convection. *Phys. Fluids* **7**, 121–134.

PROCTOR, M. R. E. 1992 Magnetoconvection. In *Sunspots: Theory and Observations* (ed. J. H. Thomas & N. O. Weiss), pp. 221–241. Kluwer.

PROCTOR, M. R. E. & MATTHEWS, P. C. 1996 $\sqrt{2}$: 1 resonance in non-Boussinesq convection. In preparation.

PROCTOR, M. R. E. & WEISS, N. O. 1982 Magnetoconvection. *Rep. Prog. Phys.* **45**, 1317–1379.

PROCTOR, M. R. E., WEISS, N. O., BROWNJOHN D. P. & HURLBURT, N. E. 1994 Nonlinear compressible magnetoconvection. Part 2. Streaming instabilities in two dimensions. *J. Fluid Mech.* **280**, 227–253.

RUCKLIDGE, A. M. & MATTHEWS, P. C. 1995*a* Analysis of the shearing instability in nonlinear convection and magnetoconvection. Submitted to *Nonlinearity.*

RUCKLIDGE, A. M. & MATTHEWS, P. C. 1995*b* Shear flow instabilities of three-dimensional magnetoconvection. In preparation.

RUCKLIDGE, A. M., SCHMIDT, H. U. & WEISS, N. O. 1995 The abrupt development of penumbrae in sunspots. *Mon. Not. R. Astron. Soc.* **273**, 491–498.

SILBER, M. & KNOBLOCH, E. 1991 Hopf bifurcation on a square lattice. *Nonlinearity* **4**, 1063–1106.

STEIN, R. F. & NORDLUND, A 1989 Topology of convection beneath the solar surface. *Astrophys. J.* **342**, L95–L98.

SPRUIT, H. C., NORDLUND, A & TITLE, A. M. 1990 Solar Convection. *Ann. Rev. Astron. Astrophys.* **28**, 263–301.

SWIFT, J. W. 1988 Hopf bifurcation with the symmetry of the square. *Nonlinearity* **1**, 333–377.

THOMAS, J. H. & WEISS, N. O. 1992 The theory of sunspots. In *Sunspots: Theory and Observations* (ed. J. H. Thomas & N. O. Weiss), pp. 3–59. Kluwer.

VAINSHTEIN, S. I., TAO, L., CATTANEO, F. & ROSNER, R. 1993 Turbulent magnetic transport effects and their relation to magnetic field intermittency. In *Theory of Solar and Planetary Dynamos* (ed. M. R. E. Proctor, P. C. Matthews & A. M. Rucklidge), pp. 311–320. Cambridge University Press.

WEISS, N. O. 1991 Magnetoconvection. *Geophys. Astrophys. Fluid Dyn.* **62**, 229–247.

WEISS, N. O. 1994 Magnetoconvective patterns. In *Solar Surface Magnetism* (ed. R. J. Rutten & C. J. Schrijver), pp. 287–295. Kluwer.

WEISS, N. O., BROWNJOHN, D. P., HURLBURT, N. E. & PROCTOR, M. R. E. 1990 Oscillatory convection in sunspot umbrae. *Mon. Not. R. Astron. Soc.* **245**, 434–452.

WHITE, D. B. 1988 The planforms and onset of convection with a temperature-dependent viscosity. *J. Fluid Mech.* **191**, 247–286.